UDK 528.481

# DETECTING IONOSPHERIC ANOMALIES ASSOCIATED WITH THREE JAPAN MIYAKO EARTHQUAKES TO SHOW THEIR CORRELATIONS AND ASSOCIATED EARTHQUAKE-INDUCED TSUNAMIS

## Lin JYH-WOEI

*Department of Earth Science, National Cheng Kung University, No.1 University Road, Taiwan*
*E-mail: pgjwl1966@gmail.com*

**Abstract.** This study employed two-dimensional principal component analysis (2DPCA) for the detection of anomalies in the two-dimensional ionospheric total electron content (TEC) associated with Japan three earthquakes and earthquake-induced tsunamis. From 04:40 to 04:50 (UTC) on February 15th, first TEC precursor was detected over the epicentre of the 16 February quake with the duration time of at least 10 minutes. A weak TEC anomaly associated with an earthquake-induced tsunami was also detected from 23:15 to 23:20 (UTC) on 16 February with the duration time of at least 5 minutes. An additional earthquake (*Mw* = 6.3) occurred in Miyako in the vicinity of the first earthquake. Second TEC precursor to the 20 February Miyako earthquake was recorded over the epicentre between 10:20 and 10:30 (UTC) on 19 February with the duration time of at least 10 minutes. A supplemental earthquake occurred (*Mw* = 6.1) as well in Miyako in the vicinity of the first earthquake. A TEC precursor to the 21 February Miyako earthquake was recorded over the epicentre between 04:15 and 04:25 (UTC) on 20 February with the duration time of at least 10 minutes. The three Miyako earthquakes presented similar anomalies and duration time in the TEC fluctuations, due largely to similarities in the magnitudes of the largest principal eigenvalues and the close proximity of the epicentres. Our results led to the reasonable confirmation that the very weak TEC anomaly following the Miyako earthquake on 16 February was associated with the earthquake-induced tsunami. 2DPCA is a useful mathematical tool for the monitoring of anomalous ionospheric fluctuations for use in the early warning of weak tsunamis.

**Keywords:** Two-Dimensional Principal Component Analysis (2DPCA), Total electron content (TEC), earthquake-induced tsunami, Miyako Earthquake, TEC precursor, early warning.

## Introduction

Recently natural precursors (e.g. electric signals) to earthquakes have been studied widely (Kamogawa 2006; Rishbeth 2006; Dautermann *et al.* 2007; Yasuda *et al.* 2009; Astafyeva, Heki 2011). A few of these studies have researched the ionospheric total electron content (TEC) anomalies associated with large earthquakes. Liu *et al.* (2004) showed that the ionospheric TEC pronouncedly decreased in the afternoon period from 12:00–18:00 (LT) and especially during the evening period from 18:00–22:00 (LT) within the five days prior to 20 M ≥ 6.0 earthquakes in Taiwan between September 1999 and December 2002. Liu *et al.* (2009) studied the TEC anomalies associated with 35 M ≥ 6.0 earthquakes that occurred from 1 May 1998 to 30 April 2008 in China. Pulinets and Tsybulyaa (2010)

found that the TEC increased for a few days prior to the Haiti earthquake with a magnitude *Mw* = 7.0 on 12 January 2010. A study by Akhoondzadeh and Saradjian (2011) used the interquartile method, wavelet transformation, and Kalman filter method to identify the TEC anomaly (decreased TEC) that appeared at 19:00 (LT) on 11 January before the Haiti earthquake. The research by Liu *et al.* (2011a) showed that a TEC anomaly with increased TEC appeared in relation to the Haiti earthquake specifically and persistently in a small region of the northern epicentre area. However, these previous studies suggested that both increased and decreased TEC could not be standard indicators of ionospheric anomalies related to earthquakes. Some studies have discussed possible causes for TEC anomalies associated with the earthquakes. Pulinets

and Boyarchuk (2004) suggested that radon emanating from active fault and crack before earthquakes ionize the atmosphere near the ground and produces large vertical electric fields. Molchanov and Hayakawa (1998) suggested gravity waves arising from small vibrations on the earth's surface lead to gas release and result in lower atmospheric turbulence and eventually ionospheric perturbations. Such small vibrations could also be responsible for gravity waves that cause anomalies, and substantial post-earthquake research has been conducted in this area (Garcia *et al.* 2005). The VAN group (Varotsos, Lazaridou 1991; Varotsos *et al.* 1998) in Greece has explored the possibility of TEC anomalies caused by stressed rocks that produce electric fields. This area of research looks at pressure stimulated currents that create electric fields in non-homogenous crustal rocks and produce seismic electric signals which the researchers attempt to recognize as earthquake precursors. Another area of study involves p-holes**.** These charge carriers are defect electrons in the $O^{2-}$ sub-lattice that are chemically equivalent to $O^-$ in a matrix of $O^{2-}$ (Pulinets *et al.* 2000; Freund 2003). They occur in stressed igneous and metamorphic rock. Pulinets and Boyarchuk (2004) suggested that lower atmospheric electric fields could travel into the ionosphere unimpeded along geomagnetic lines and cause TEC anomalies. Occhipinti *et al.* (2011) described the tsunami following the Mw = 9.0 Tohoku earthquake that occurred at 05:46 (UT) on 11 March 2011. This earthquake produced internal gravity waves into the neutral atmosphere and large disturbances in the overlying ionospheric plasma while propagating through the Pacific Ocean. The effects of tsunamis that propagate from the epicentre to the ionosphere were demonstrated by Makela *et al.* (2011). Tsugawa *et al.* (2011) and Saito *et al.* (2011) investigated the TEC maps of Japan for the Tohoku Earthquake and showed that the TEC variation appeared approximately seven minutes after the earthquake occurrence. In this study, two-dimensional principal component analysis (2DPCA) is performed to detect TEC anomalies associated with three Miyako earthquakes occurred on 16, 20 and 21 February 2015 in Japan and their associated earthquake-induced tsunamis. The epicentres of the three earthquakes are very close. TEC data during the time period from 5 days before Miyako earthquake on February 16 to 06:00 on 20 February 2015 were processed. During this examined time period, a Miyako earthquake occurred on 20 February. TEC data after last two earthquakes were processed to detect earthquake-induced tsunami TEC

anomalies because the epicentres locate in the sea near Japan Trench (U.S. Geological Survey). The first Miyako earthquake was the *Mw* = 6.7 Miyako earthquake that occurred in Japan at 23:06:27 (UTC) on 16 February 2015. The epicentre was 39.830°N, 142.890°E and the depth was 23.0 km. The second Miyako earthquake was the *Mw* = 6.3 Miyako earthquake that occurred in Japan at 04:25:24 (UTC) on 16 February 2015. The epicentre was 39.847°N, 143.569°E and the depth was 13.5 km. The third Miyako earthquake was the *Mw* = 6.1 Miyako earthquake that occurred in Japan at 10:13:54 (UTC) on 21 February 2015. The epicentre was 39.863 °N, 143.425 °E and the depth was 10.0km (U.S. Geological Survey). Their epicentres have the close proximity. The TEC data of 5-day time period before the first Miyako earthquake were processed because TEC precursors have usually been identified during this period before large earthquakes (Liu *et al.* 2006).

## 1. TEC Data Source

The Global Differential GPS (GDGPS) system is a complete, highly accurate, and extremely robust real-time GPS monitoring and augmentation system. Employing a large ground network of real-time reference receivers, innovative network architecture, and award-winning real-time data processing software, the GDGPS system provides decimetre (10 cm)-scale positioning accuracy and subnanosecond-scale time transfer accuracy on ground, in air, and in space, independent of local infrastructure. A complete array of real-time GPS state information, environmental data, and ancillary products are available in support of the most demanding GPS augmentation operations – Assisted GPS (A-GPS) services, situational assessment, and environmental monitoring – globally, uniformly, accurately, and reliably. The global TEC data were real-time measured by the sensors (receivers) in the Global Differential GPS satellites, and then they were sent back to this network. The spatial resolution of the TEC data for GDGPS system is based on real-time dual frequency measurements from its vast global tracking network (real-time tracking network on the ground), and the GDGPS System produces two dimensional total electron content (TEC) values on a 2°×2° global grid every 5 minutes (Yoaz, Byron 2014). The estimated TEC data have been corrected for biases during measurements of dual-frequency delays of GPS signals e.g. carrier phase biases, satellite state corrections, ionospheric delay and troposphere, which need

to be removed using ground-based post-processing software (Raman, Garin 2005; Wu, Bar-Sever 2005).

## 2. Method

2DPCA is a good method that can removed small sample signal size (SSS) problem (Lin 2013, 2014) when TEC data are two dimensional data. The PCA converts the measurements into one-dimensional TEC data before covariance matrix calculation. The covariance matrix of PCA is based on an input matrix with the dimension of $m \times n$, which is reshaped from one-dimensional data (length of $m$ multiplying $n$). Reshaping data will cause computing error because PCA is a tool to deal with one-dimensional data. That proclaims the spatial structure and information can not be well preserved due to some original information loss when inverting to original dimension under the condition of the matrix being small sample size (SSS).

## 3. TEC Data Processing

We used 2DPCA to process TEC data associated with time periods that had previously been examined thoroughly. TEC anomalies associated with the two Miyako earthquakes and the subsequent tsunamis could not be identified using the largest principal eigenvalues. However, TEC anomalies were detected using the largest principal eigenvalues during the three time periods from 04:40:00 to 04:50:00 (UTC) on 15 February, from 23:15 to 23:20 (UTC) on 16 February, and from 10:20 to 10:30 (UTC) on 19 February 2015. The procedures used in the processing of TEC data in the three periods are presented in this study. Figure 1(a) presents the GIMs in these three time periods. With the exception of equatorial ionization anomalies (EIA), other TEC anomalies in the world could not be easily observed without the help of 2DPCA. The TEC data of the global region in Figure 1(a) are divided into 600 grids 12° and 9° in longitude and latitude, respectively.

Thus, the size of each grid is 12° in longitude and 9° in latitude. For convenience, the terminology grid is used instead of area in this study. Section Two referred to the contents regarding the spatial resolution of the TEC data for the GDGPS system. A grid with 6 TEC data points associated with Longitude and 4 with the Latitude would include approximately 24 TEC data points. Using 2DPCA for the computation of 600 grids with 24 TEC data points would incur considerable computational resources. Our results, obtained using 2DPCA with only 4 TEC data points in each grid, were nearly the same as those obtained using a grid of 600.

This allows that when performing 2DPCA, the quality of TEC data processing was not distorted taking 4 TEC data (low dimensional data) instead of 24 TEC data (high dimensional data) in each grid. Therefore, we opted for this configuration in this study. When performing a quantitative analysis by 2DPCA, 4 TEC data are used in each grid to form a matrix $A$, and this matrix is then input into Equation (1) with the dimensions of $2 \times 2$. The matrix has a small sample signal size (SSS). Eqs (2)–(4) are performed and then the principal eigenvalue of $G$ is estimated. The largest principal eigenvalue in the grid that includes the epicentre of the earthquakes was assigned to a TEC anomaly associated with an earthquake or earthquake-induced Tsunami. This allows the principal eigenvalues to be computed for each of the 600 grids in the world. Therefore, Figure 1(b) can be explained as a result in a principal eigenvalue in a grid which is indicated principal spatial characteristics, pattern and situation of the TEC data in this grid. However, for ease of presentation, each grid is filled uniformly with colour to indicate principal spatial characteristics, patterns, and the conditions associated with each grid.

This study has shown the largest principal eigenvalue for a grid incl. the epicentre of the Miyako earthquake in Japan. A principal eigenvalues was assigned to the principal spatial characteristics of the TEC data in a grid. A largest principal eigenvalue in a grid incl. the epicentre of Miyako earthquake (February 16) during 04:40 to 04:50 (UTC) on 15 February 2015 was assigned to the principal spatial characteristics of the TEC data in this grid. The largest principal eigenvalue indicated the earthquake- associated TEC anomaly. During 23:15 to 23:20 (UTC) on 16 February 2015, a largest principal eigenvalue was assigned to the principal spatial characteristics of the TEC data in a grid. This largest principal eigenvalue indicated the earthquake-induced tsunami TEC anomaly. A largest principal eigenvalue in a grid incl. the epicentre of Miyako earthquake (February 20) during 10:20 to 10:30 (UTC) on 19 February 2015 was assigned to the earthquake-associated TEC anomaly.
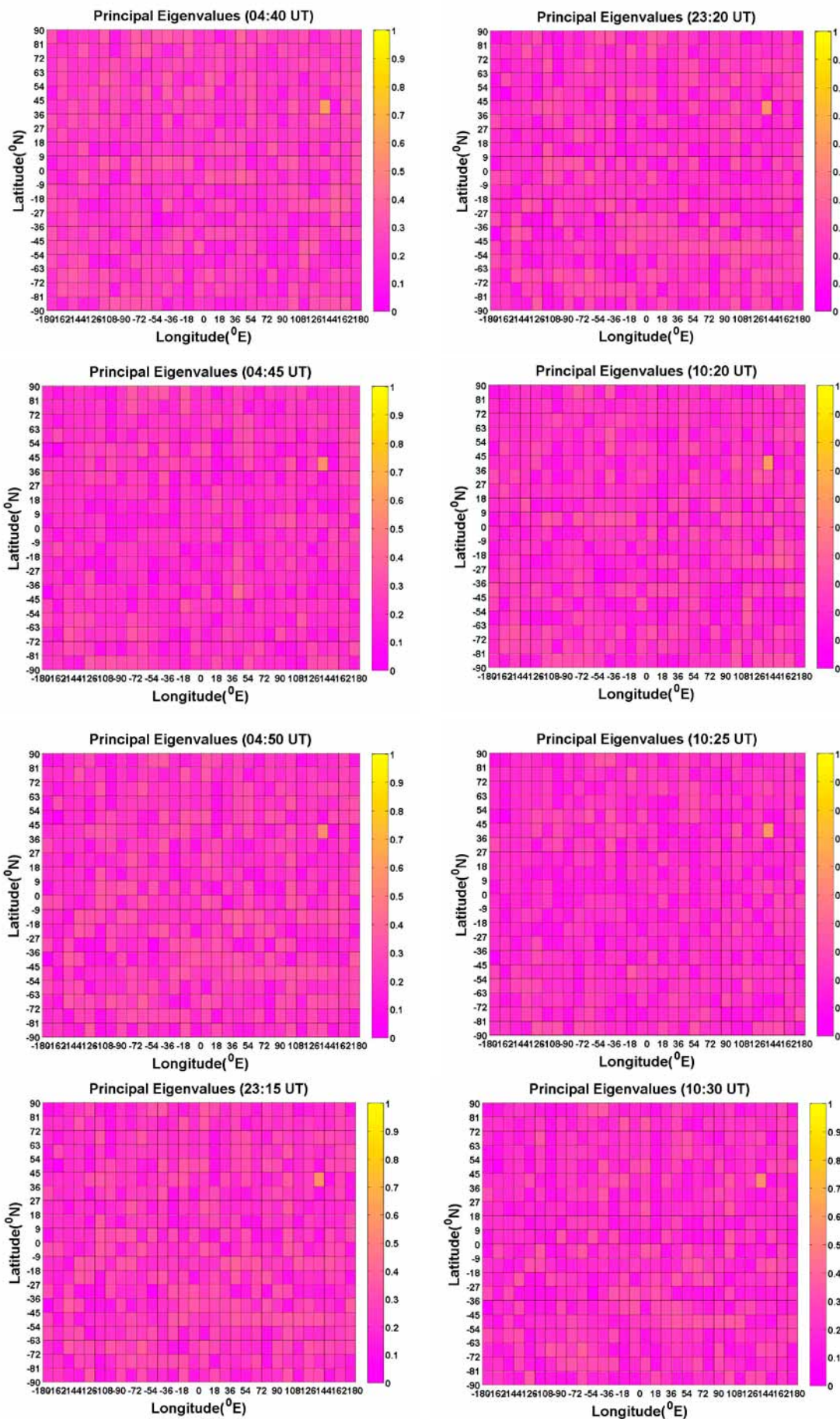
## 4. Results

This study has shown the largest principal eigenvalues in a grid that includes the epicentres of two earthquakes in three time periods. This asserted that other TEC anomalies (e.g. the equatorial ionization anomaly (EIA) and non-earthquake-associated TEC anomalies, and other earthquake-associated TEC anomalies in the
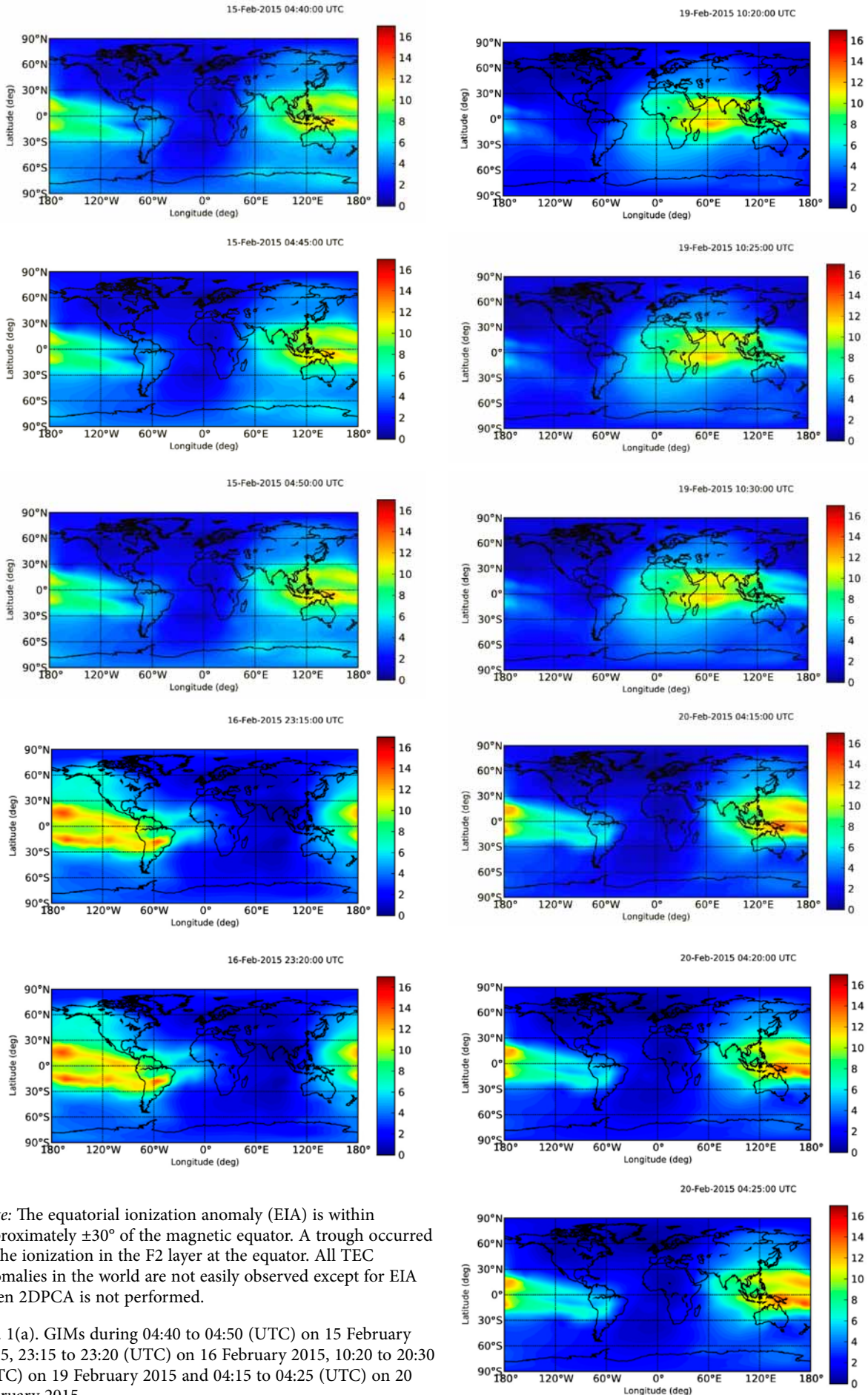
*Note:* The equatorial ionization anomaly (EIA) is within approximately ±30° of the magnetic equator. A trough occurred in the ionization in the F2 layer at the equator. All TEC anomalies in the world are not easily observed except for EIA when 2DPCA is not performed.

Fig. 1(a). GIMs during 04:40 to 04:50 (UTC) on 15 February 2015, 23:15 to 23:20 (UTC) on 16 February 2015, 10:20 to 20:30 (UTC) on 19 February 2015 and 04:15 to 04:25 (UTC) on 20 February 2015
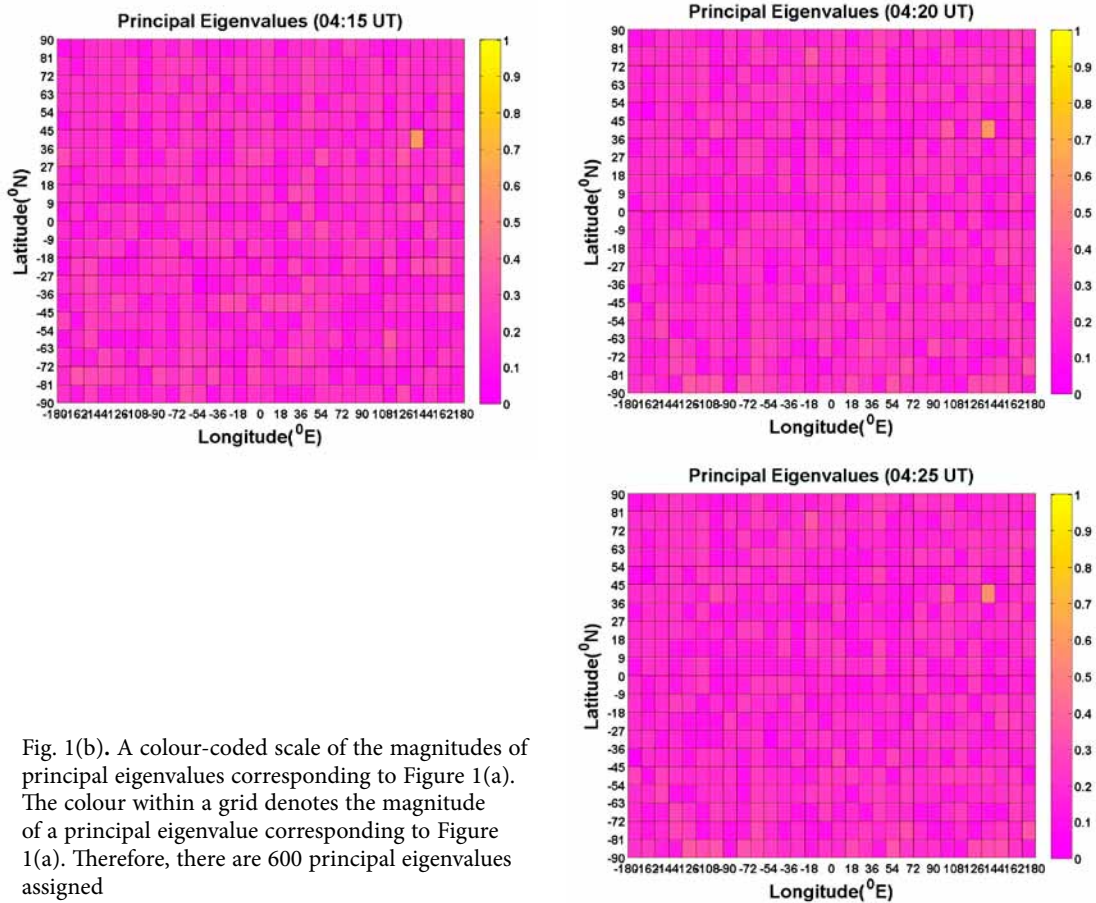
Principal Eigenvalues (04:40 UT)

Principal Eigenvalues (23:20 UT)

Principal Eigenvalues (04:45 UT)

Principal Eigenvalues (10:20 UT)

Principal Eigenvalues (04:50 UT)

Principal Eigenvalues (10:25 UT)

Principal Eigenvalues (23:15 UT)

Principal Eigenvalues (10:30 UT)

→

→



**Fig. 1(b).** A colour-coded scale of the magnitudes of principal eigenvalues corresponding to Figure 1(a). The colour within a grid denotes the magnitude of a principal eigenvalue corresponding to Figure 1(a). Therefore, there are 600 principal eigenvalues assigned

meantime and non-earthquake-induced tsunami TEC anomalies) were already suppressed resulting in smaller principal eigenvalues during the entire examined time period with the exception of the previous three time periods, such that the largest principal eigenvalue of 2DPCA should match the pattern of TEC anomalies associated with the earthquake or earthquake-induced tsunami. Therefore, by performing 2DPCA, the earthquake-associated and the earthquake-induced Tsunami TEC anomalies could be distinguished from other TEC anomalies in the previous three time periods. This is an advantage of 2DPCA. The possibility of other factors such as solar flare and geomagnetic effects affecting the results are considered by examining $K_p$ indices. February, 15, 16 and 19 and 20 were geomagnetic quiet days shown in Figure 2 ($K_p < 4$) (Bartels 1957; Elliott *et al.* 2013). The $K_p$ index shown in Figure 2 is calculated as a weighted average of K-indices from a network of geomagnetic observatories. The $K_p$ index allows for disturbances in the horizontal component of earthXs magnetic field to be represented on a scale of 0–9, with 1 indicating calmness and 5 or more indicating a geomagnetic storm. Therefore,

February, 15, 16, 19 and 20 was a geomagnetic quiet day with $K_p < 4$.

## 5. Discussion

2DPCA was able to detect a TEC precursor of Miyako earthquake on 16 February during the time periods from 04:40 to 04:50 (UTC) on 15 February with the duration time of at least 10 minutes. The earthquake-induced tsunami TEC anomaly was detectable during the time period from 23:15 to 23:20 (UTC) on 16 February with the duration of at least 5 minutes. Another TEC precursor of Miyako earthquake on 20 February during the time period from 10:20 to 10:30 (UTC) on 19 February was detectable with the duration time of at least 10 minutes. Additionally, TEC precursor of Miyako earthquake on 21 February during the time period from 04:15 to 04:25 (UTC) on 20 February was detectable with the duration time of at least 10 minutes. The three Miyako earthquakes presented similar anomalies in the TEC fluctuations, due largely to similarities in the magnitudes and duration time of the largest principal eigenvalues and the close proximity of the epicentres. 2DPCA may be a useful

and reasonable tool to confirm that the earthquakes on 20 and 21 February were an aftershock of initial event by observing the characteristics of largest principal eigenvalues. These events were not Earthquake swarms. The TEC anomaly associated with the Miyako earthquake-induced tsunamis on 20 and 21 February were not detectable because the magnitude of this earthquake was negligible, as confirmed by information broadcast from the National Tsunami Warning Center and Pacific Tsunami Warning Center. However, this is worthy of future investigation. Gravity waves causing the TEC precursors could not be possible because vibration in the Earth's surface before this earthquake would be minimal when these vibrations are assumed as the precursors. Gravity waves causing the tsunami should be possible. However, the true mechanism that causes the TEC precursors from the earthquake is not easily determined. However, some reasons were introduced in Section one. This study has reasonably confirmed that a TEC anomaly associated with the earthquake-induced tsunami during the time period from 23:15 to 23:20 (UTC) appeared on 16 February approximately 9 minutes after Miyako earthquake on 16 February. This TEC anomaly should be a very weak earthquake-induced tsunami TEC anomaly although the National Tsunami Warning Center reported that there was no tsunami danger for the U.S. West Coast, British Columbia, or Alaska. Based on earthquake information and historic tsunami records, this earthquake was insufficient to generate a tsunami. As stated in Section one, Tsugawa *et al.* (2011) and Saito *et al.* (2011) showed that the TEC anomaly appeared approximately 7 minutes after the earthquake occurrence. Approximately 9 minutes after Miyako earthquake on 16 February should be a reasonable result because this earthquake induced a weak earthquake-induced tsunami TEC anomaly. The time period of the earthquake-induced tsunami TEC anomaly was very short. Results demonstrate that 2DPCA should be sensitive enough to detect weak earthquake-induced tsunami TEC anomaly. 2DPCA is a useful mathematical tool for monitoring the propagation of ionospheric anomalous fluctuation because ionospheric anomalous fluctuation propagation speed is faster than earthquake-induced tsunami spreading speed. This tool can serve as detecting a weak tsunami. Therefore strong tsunamis could also be detectable. Thus early warning of tsunamis, such as the case study of the Tohoku Earthquake (Liu *et al.* 2011b; Lin 2015), is possible using this tool.
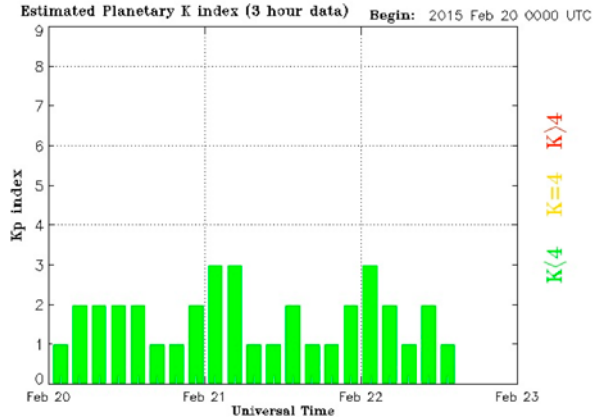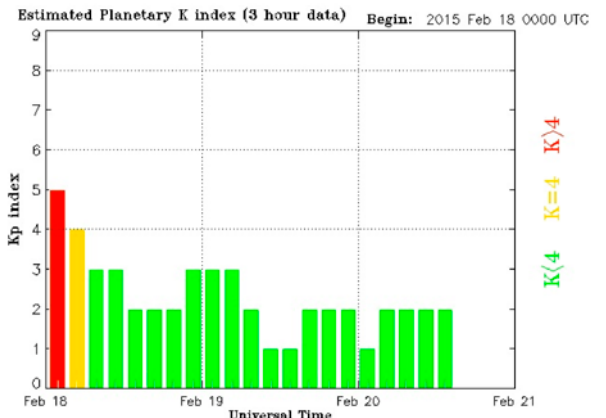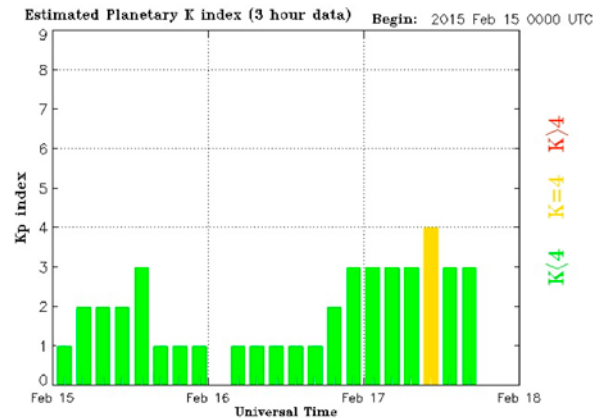


*Note:* The $K_p$ index is calculated as a weighted average of K-indices from a network of geomagnetic observatories. The $K_p$ index allows for disturbances in the horizontal component of earthXs magnetic field to be represented on a scale of 0–9, with 1 indicating calmness and 5 or more indicating a geomagnetic storm.
Therefore, February 15, 16, 19 and 20 were geomagnetic quiet days with $K_p < 4$.

Fig. 2. $K_p$ indices from 00:00 (UT) on 18 to 18:00 (UT) on 17 in February 2015 (Space Weather Prediction Center)

## 6. Conclusion

A TEC precursor was detected for the Miyako earthquake occurred at 23:06:27 (UTC) on 15 February 2015 for a period of 10 minutes from 04:40 to 04:50 (UTC) on 15 February 2015. The earthquake-induced weak tsunami TEC anomaly was detected during the time period from 23:15 to 23:20 (UTC) on 16 February 2015 with the duration time of at least 5 minutes. Another TEC between 10:20 and 10:30 (UTC) on 19 February 2015 was identified as a precursor to the Miyako earthquake on 20 February 2015. A TEC anomaly related to the earthquake on 21 February 2015 was identified as precursor between 04:15 and 04:15 (UTC) on 20 February 2015. The characteristics of their largest principal eigenvalues have confirmed the high correlations between these three earthquakes. However, these events were not Earthquake swarms. Detecting a TEC anomaly associated with the Miyako earthquake-induced tsunami is unable for the earthquakes on 20 and 21 February 2015, as confirmed in reports filed by the National Tsunami Warning Center and Pacific Tsunami Warning Center. 2DPCA is a useful mathematical tool for monitoring the propagation of ionospheric anomalous fluctuations and serve as an early warning of impending tsunami. Fluctuations in TEC anomalies associated with the two Miyako earthquakes should be similar, due to the fact that the magnitudes of their largest principal eigenvalues were nearly the same. Thus, it would be reasonable to assume that they should be highly correlated and present similar source mechanisms.

## Acknowledgements

## References

Akhoondzadeh, M.; Saradjian, M. R. 2011. TEC variations analysis concerning Haiti (January 12, 2010) and Samoa (September 29, 2009) earthquakes, *Advances in Space Research* 47(1): 94–104. http://dx.doi.org/10.1016/j.asr.2010.07.024

Astafyeva, E.; Heki, K. 2011. Vertical TEC over seismically active region during low solar activity, *Journal of Atmospheric and Solar-Terrestrial Physics* 73(13): 1643–1652. http://dx.doi.org/10.1016/j.jastp.2011.02.020

Bartels, J. 1957. The technique of scaling indices K and Q of geomagnetic activity, *Annales of the International Geophysical Year* 4: 215–226.

Dautermann, T.; Calais, E.; Haase, J.; Garrison, J. 2007. Investigation of ionospheric electron content variations before earthquakes in southern California, 2003–2004, *Journal of Geophysical Research* 112: B02106. http://dx.doi.org/10.1029/2006JB004447

Elliott, H. A.; Jahn, J.-M.; McComas, D. J. 2013. The Kp index and solar wind speed relationship: insights for improving space weather forecasts, *Space Weather* 11(6): 339–349. http://dx.doi.org/10.1002/swe.20053

Freund, F. T. 2003. Rocks that crackle and sparkle and glow strange pre-earthquake phenomena, *Journal of Scientific Exploration* 17(1): 37–71.

Garcia, R.; Crespon, F.; Ducic, V.; Lognonné, P. 2005. Three-dimensional ionospheric tomography of post-seismic perturbations produced by the Denali earthquake from GPS data, *Geophysical Journal International* 163(3): 1049–1064. http://dx.doi.org/10.1111/j.1365-246X.2005.02775.x

Kamogawa, M. 2006. Preseismic lithosphere-atmosphere-ionosphere coupling, *Eos Transactions, American Geophysical Union* 87(40): 417. http://dx.doi.org/10.1029/2006EO400002

Lin, J. W. 2013. Ionospheric anomaly related to M = 6.6, 26 August 2012, Tobelo earthquake near Indonesia: two-dimensional principal component analysis, *Acta Geodaetica et Geophysica* 48(3): 247–264. http://dx.doi.org/10.1007/s40328-013-0024-6

Lin, J. W. 2014. Ionospheric precursor for a deep earthquake (~378 km) near Papua New Guinea occurred on 7 July 2013, Mw = 7.2 in the environment of geomagnetic storm using two-dimensional principal component analysis (2DPCA), *NGRK Georisk: Assessment and Management of Risk for Engineered Systems and Geohazards* 8(2): 141–146. http://dx.doi.org/10.1080/17499518.2014.880853

Lin, J. W. 2015. Early warning of tsunami from seismo-ionospheric fluctuation after Japan's March 11, 2011, M = 9.0 Tohoku earthquake using two-dimensional principal component analysis. *Annals of Geophysics* 58(4): A0442.

Liu, J. Y.; Chen, Y. I.; Chuo, Y. J.; Chen, C. S. 2006. A statistical investigation of pre-earthquake ionospheric anomaly, *Journal of Geophysical Research* 111: A05304.

Liu, J. Y; Chen, Y. I.; Chen, C. H.; Liu, C. Y; Chen, C. Y.; Nishihashi, M.; Li, J. Z., *et al.* 2009. Seismoionospheric GPS total electron content anomalies observed before the 12 May 2008 Mw = 7.9 Wenchuan Earthquake, *Journal of Geophysical Research* 114(A4). http://dx.doi.org/10.1029/2008JA013698

Liu, J. Y.; Chuo, Y. J.; Shan, S. J.; Tsai, Y. B.; Chen, Y. I.; Pulinets, S. A.; Yu, S. B. 2004. Pre-earthquake ionospheric anomalies registered by continuous GPS TEC measurements, *Annals of Geophysics* 22(5): 1585–1593. http://dx.doi.org/10.5194/angeo-22-1585-2004

Liu, J. Y.; Le, H.; Chen, Y. I. 2011a. Observations and simulations of seismoionospheric GPS total electron content anomalies before the 12 January 2010 M7 Haiti earthquake, *Journal of Geophysical Research* 116: A04302. http://dx.doi.org/10.1029/2010JA015704

Liu, J. Y.; Chen, C. H.; Lin, C. H.; Tsai, H. F.; Chen, C. H.; Kamogawa, M. 2011b. Ionospheric disturbances triggered by the 11 March 2011 M9.0 Tohoku earthquake, *Journal of Geophysical Research* 116: A06319. http://dx.doi.org/10.1029/2011JA016761

Makela, J. J.; Lognonné, P.; Hébert, H.; Gehrels, T.; Rolland, L.; Allgeyer, S.; Kherani A.; Occhipinti, G.; Astafyeva, E.; Coïsson, P.; Loevenbruck, A.; Clévédé, E.;

Kelley, M. C.; Lamouroux, J. 2011. Imaging and modeling the ionospheric airglow response over Hawaii to the tsunami generated by the Tohoku earthquake of 11 March 2011, *Geophysical Research Letters* 38: L00G02. http://dx.doi.org/10.1029/2011GL047860

Molchanov, O. A.; Hayakawa, M. 1998. Subionospheric VLF signal perturbations possibly related to earthquakes, *Journal of Geophysical Research* 103(A8): 17489–17504. http://dx.doi.org/10.1029/98JA00999

Occhipinti, G.; Coisson, P.; Makela, J. J.; Allgeyer, S. 2011. Three-dimensional numerical modeling of tsunami-related internal gravity waves in the Hawaiian atmosphere, *Earth Planets Space* 63: 847–851. http://dx.doi.org/10.5047/eps.2011.06.051

Pulinets, S. A.; Boyarchuk, K. A.; Hegai, V. V.; Kim, V. P.; Lomonosov, A. M. 2000. Quasielectrostatic model of atmosphere-thermosphereionosphere coupling, *Advances in Space Research* 26(8): 1209–1218. http://dx.doi.org/10.1016/S0273-1177(99)01223-5

Pulinets, S.; Boyarchuk, K. 2004. *Ionospheric precursors of earthquakes.* Berlin, Heidelberg: Springer-Verlag. 315 p.

Pulinets, S. A.; Tsybulyaa, K. G. 2010. Unique variations of the total electron content in the preparation period of Haitian Earthquake (M7.0) on January 12, 2010, *Geomagnetism and Aeronomy* 50(5): 686–689. http://dx.doi.org/10.1134/S0016793210050166

Raman, S.; Garin, L. 2005. *Performance evaluation of Global Differential GPS (GDGPS) for single frequency C/A code receivers.* SiRF Technology, Inc.

Rishbeth, H. 2006. Ionoquakes: Earthquake precursors in the ionosphere? *Eos Transactions, American Geophysical Union* 87(32): 316. http://dx.doi.org/10.1029/2006EO320008

Saito, T.; Ito, Y.; Inazu, D.; Hino, R. 2011. Tsunami source of the 2011 Tohoku-Oki earthquake, Japan: Inversion analysis based on dispersive tsunami simulations, *Geophysical Research Letter,* 38 L00G19. http://dx.doi.org/10.1029/2011GL049089

Tsugawa, T.; Saito, A.; Otsuka, Y.; Nishioka, M.; Maruyama, T.; Kato, H.; Nagatsuma, T.; Murata, K. T. 2011. Ionospheric disturbances detected by GPS total electron content observation after the 2011 off the Pacific coast of Tohoku Earthquake, *Earth Planets Space* 63: 875–879. http://dx.doi.org/10.5047/eps.2011.06.035

Wu, S.; Bar-Sever, Y. 2005. Real-time sub-cm differential orbit determination of two low-earth orbiters with GPS bias fixing jet propulsion laboratory. USA: California Institute of Technology.

Yasuda, Y.; Ida, Y.; Goto, T.; Hayakawa, M. 2009. Interferometric direction finding of over-horizon VHF transmitter signals and natural VHF radio emissions possibly associated with earthquakes, *Radio Science* 44, RS2009. http://dx.doi.org/10.1029/2008RS003884

Yoaz, E.; Bar-Sever, Y.; Byron, A. I. 2014. *Patent application title: Enhanced broadcast ephemeris for high accuracy assisted GPS positioning.* California Institute of Technology. IPC8 Class: AG01S1927FI. USPC Class: 34235766. Patent application number: 20140077991.

Varotsos, P.; Lazaridou, M. 1991. Latest aspects of earthquake prediction in Greece based on seismic electric signals, *Tectonophysics* 188: 322.

Varotsos, P. A.; Sarlis, N. V.; Lazaridou, M.; Kapiris, P. 1998. Transmission of stress induced electric signals in dielectric media, *Journal of Applied Physics* 83: 60–70. http://dx.doi.org/10.1063/1.366702

**Lin JYH-WOEI.** Master Degree in Institute of Geophysics, National Central University, Taiwan. PhD from 1996, in Institut für Geophysik, Technische Universität Clausthal, Germany. Research interests: Space Physics, Geosciences, Geodesy, Back Propagation Neural Network, Physics.